

## A High-Current-Density Terahertz Electron-Optical System Based on Carbon Nanotube Cold Cathode

Journal:	<i>Transactions on Electron Devices</i>
Manuscript ID	TED-2020-06-1295-R
Manuscript Type:	Regular
Date Submitted by the Author:	18-Jun-2020
Complete List of Authors:	Gu, Yunlong; University of Electronic Science and Technology of China, School of Electronic Science and Engineering Yuan, XueSong; University of Electronic Science And Technology of China, School of Physical Electronics Xu, Xiaotao; University of Electronic Science and Technology of China, School of Electronic Science and Engineering Cole, Matt; University of Bath, Electronic & Electrical Engineering Chen, Qingyun; University of Electronic Science and Technology of China, School of Electronic Science and Engineering Zhang, Yu; Sun Yat-sen university, School of Physics and Engineering Wang, Bin; University of Electronic Science and Technology of China, School of Physical Electronics Li, Hailong; University of Electronic Science and Technology of China, Yin, Yong; University of Electronic Science and Technology of China, School of Physical Electronics Yan, Yang; University of Electronic Science and Technology of China, School of Physical Electronics
Area of Expertise:	Terahertz, high-current-density, gyrotron, mode competition, high-order-harmonic, carbon nanotube, cold cathode

**SCHOLARONE™**  
Manuscripts

# A High-Current-Density Terahertz Electron-Optical System Based on Carbon Nanotube Cold Cathode

Yunlong Gu, Xuesong Yuan, Xiaotao Xu, Matthew T. Cole, Qingyun Chen, Yu Zhang, Bin Wang, Hailong Li, Yong Yin, and YangYan

**Abstract**—A high-current-density terahertz electron-optical system based on a carbon nanotube (CNT) cold cathode has been investigated in order to solve notable mode competition in high order harmonic gyrotrons. Simulation results show that a near-axis electron beam can be generated, with beam current of 160mA at an accelerating voltage of 23.5kV. The source supports electron beam with velocity ratio of 1.1 and a guiding center radius of 57  $\mu$ m. A narrow beam spatial distribution is evidenced by adjusting control anode voltage, satisfying the need for high operating current density in slow wave devices. The current density of the electron beam is up to 620 A/cm<sup>2</sup> and the velocity ratio is 0.44, with parallel energy accounts for 84% of the total energy.

**Index Terms**—Terahertz, high-current-density, gyrotron, mode competition, high-order-harmonic, carbon nanotube, cold cathode.

## I. INTRODUCTION

Driving the rapid development of terahertz science and technology, terahertz radiation sources have found wide use in radar, communications, and biomedical applications [1-2]. Compared with the solid-state sources, vacuum electron radiation sources (VERS) offer advantageously high output powers (up to 1 GW) and high operating frequencies (up to 1 THz), making them well-suited to the demanding requirements of industry and commerce [3]. Gyrotron structures, fast-wave devices with some of the highest recorded output powers, have received extensive attention in space communication, thermonuclear fusion, and medical diagnosis [4-11]. In such devices, affordable and movable scale magnets can generate magnetic fields of 10-15 T, which corresponds to electron-cyclotron frequencies of 0.3-0.4 THz [12]. Nevertheless, such magnets remain bulky and

This work was supported by the National Key Research and Development Program of China (No.2019YFA0210202), National Natural Science Foundation of China (No.61771096), and Fundamental Research Funds for the Central Universities (No. ZYGX2019J012, No. ZYGX2019Z006).

Yunlong Gu, Xuesong Yuan, Xiaotao Xu, Qingyun Chen, Bin Wang, Hailong Li, Yong Yin and Yang Yan are with the School of Electronic Science and Engineering, University of Electronic Science & Technology of China, Chengdu 610054 China (Correspondence e-mail: yuanxs@uestc.edu.cn).

Matthew T. Cole is with the Department of Electronic & Electrical Engineering, University of Bath, Bath, BA2 7AY, United Kingdom (e-mail: m.t.cole@bath.ac.uk).

Yu Zhang is with the State Key Laboratory Optoelectronic Materials & Technologies, Sun Yat-Sen University, Guangzhou 510275 China (e-mail: stszhyu@mail.sysu.edu.cn).

account for significant volumes within present designs. Reducing the magnet size deleteriously reduces the attainable magnetic field, and in doing so compromises the device functionality. However, the required magnetic field, and hence magnet dimensions, can be greatly decreased by engineering high-order harmonic operation. Nevertheless, mode competition hinders the development of gyrotrons when operating at high-order harmonic. A third harmonic gyrotron with axis-encircling electron beam (large-orbit gyrotron), operating at 1 THz, has recently been developed [13]. One solution to mode competition is decreasing the electron beam radius. As the radius of the electron beam becomes increasing small, there is significant mode depletion, resulting in only the TE<sub>25</sub> mode to participate in mode competition. However, the design of such electron-optical system is relatively complex, require fine machining, accurate modelling, and careful assembly, especially within the magnetic field system [14].

By increasing the operating frequency (up to terahertz frequency band) the minimum working current density of traditional terahertz VERS systems increases dramatically, typically to hundreds of A/cm<sup>2</sup>. The minimum current density for some electron tubes, such as Ledatrons, Travelling Wave Tubes (TWTs), Reflex Klystrons, and Backward Wave Oscillators (BWO) are 330A/cm<sup>2</sup>, 70A/cm<sup>2</sup>, 216A/cm<sup>2</sup>, 874A/cm<sup>2</sup>, respectively [15-17]. Despite significant research efforts, such large minimum current densities continue to plague the development of traditional VERS systems. Due to their cost, ease of access, and technological maturity, almost all commercial VERS continue to employ thermionic cathodes as the electron emission sources. Nevertheless, thermionic cathodes suffer from significant functional limitations, such as the need for high operating temperatures which limits system design opportunities due to thermal dissipation challenges, large operating volume, and comparatively slow response times [18-20]. Conversely, field electron emission cold cathodes support almost instantaneous turn-on, the ability to create ultra-compact designs, tolerance towards small working volumes which relaxes system evacuation requirements, and the ability to operate at near-room-temperature. As a result, field electron emission cold cathodes are coming to the fore as a leading alternative electron emission technology in a new generation of VERS [21-22]. Supported by the emergence of new types of 1D and 2D nanomaterials, field electron emission systems based on carbon nanotubes (CNTs) have been widely demonstrated to provide high emission current densities, excellent chemical, thermal and temporal stability, and low opening fields, making them a prime candidate for use in a

variety of electron emission systems, including display devices, microwave sources and X-ray tubes [23-29].

In this paper, a high-current-density terahertz electron-optical system based on CNTs is theoretically and experimentally investigated. Here we demonstrate the potential of CNT-based field emission sources as a candidate technology for both fast wave devices, such as gyrotrons, as well as slow wave devices, such as TWTs, Klystrons, and BWOs. In this work a near-axis small orbit electron beam has been obtained. We show that mode competition can be solved using such a system, which offers a guiding center radius of only 57  $\mu\text{m}$  at the 0.6 THz third harmonic  $\text{TE}_{37}$  mode gyrotron. Meanwhile design sensitivity to the control anode voltage and magnetic field spatially localized to the cathode have been investigated, with beam current densities of 620  $\text{A}/\text{cm}^2$  having been achieved, satisfying the demands of state of the art slow wave devices.

## II. DESIGN AND SIMULATION

In this section, we describe the design of the electron-optical system based on a CNT cold cathode. This section explores the cathode, control anode and accelerating anode. Particle in cell (PIC) simulation has been used throughout to investigate the electron-optical system. Efforts have focused on explicating design sensitivity to control anode voltage and magnetic field in the immediate emission volume. Simulations are based on direct experimental findings from CNTs cold cathodes. To form the electron emitter, CNTs were synthesised on a 0.1 mm diameter Ni80Cr20 alloy wire substrates, outlined in Ref. [30]. The experimental results demonstrate a maximum operating emission current density of 7.65  $\text{A}/\text{cm}^2$  at 2.13 kV/mm, indicating the CNTs suitability to operate as the emission source in high-current-density terahertz electron-optical systems. To obtain the field emission parameters required for the present technology, dual Ni80Cr20 alloy wires were joined to form a ring emitter, which was subsequently embedded within a rectangular groove within the system. A SEM (scanning electron microscope) image of the coated Ni80Cr20 wire, and the synthesized CNT thin film are shown in Fig.1 with a CAD rendering of the toroidal electron emission subsystem.

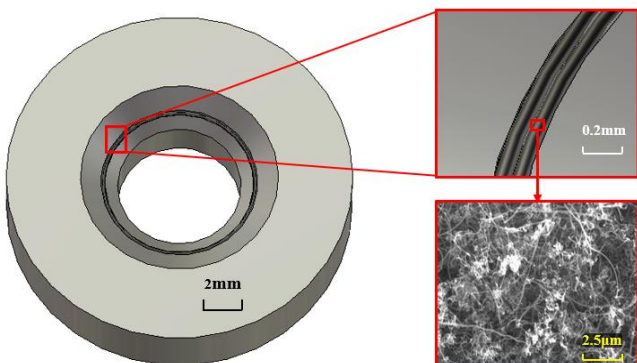


Fig.1. simulation structure of dual joined Ni80Cr20 alloy wires. Inset: detailed view of dual Ni80Cr20 alloy wires and areal-view SEM image of the CNT thin film adapted from Ref. [30].

In order to obtain the field emission parameters of the CNT cold cathode, the emission current density is fitted to established empirical data using the simplified Fowler-Nordheim (FN) equation:

$$J = A'E^2 \exp(-B'/E) \quad (1)$$

where  $A'$  and  $B'$  are the field emission coefficient,  $A' = 2.17 \times 10^{-4} \text{A}/\text{V}^2$  and  $B' = 2.02 \times 10^7 \text{V}/\text{m}$  have been determined by numerical fitting on the basis of our experimental data in Ref. [30] and [31]. For the 0.1mm Ni80Cr20 alloy wire, we find that the simulation mesh must be set to at least 0.01mm in order to obtain accurate and empirically representative results. This mesh size is far smaller than the electron-optical system (8mm  $\times$  310mm), which makes it difficult to directly integrate the alloy wires in a comparatively large volume. In our simulations, as a result, we approximate the dual Ni80Cr20 alloy wires as an equivalent red annular surface emitting band with width of 0.2mm, as shown in the inset of Fig. 2. Meshes have been investigated using 3D and 2.5D PIC simulation software to analyse the computationally demanding spatial and temporal evolution of the electron beam. The field emission coefficient of the simulation model with annular surface emitting band  $A''$  and  $B''$  were numerically fitted according to the simulation data of dual Ni80Cr20 alloy wires, where  $A'' = 2.15 \times 10^{-4} \text{A}/\text{V}^2$  and  $B'' = 2.03 \times 10^7 \text{V}/\text{m}$ .

The annular surface emitting band simulations (3D and 2.5D) and dual Ni80Cr20 alloy wires (3D) and its fitting, are shown in Fig.2. Empirical data and equivalent 3D and 2.5D models align well, attesting that our model approximations are valid.

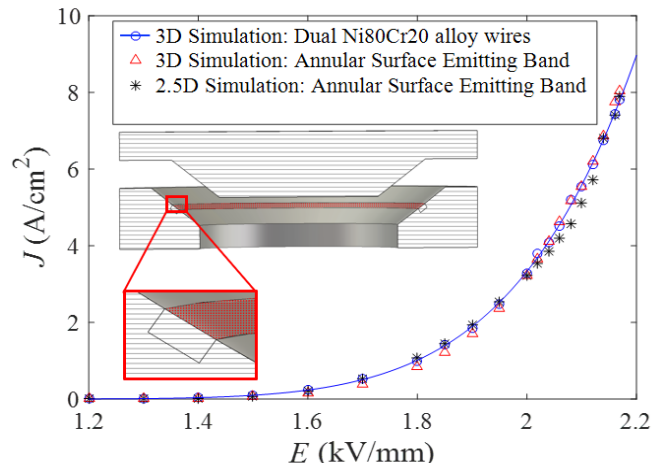


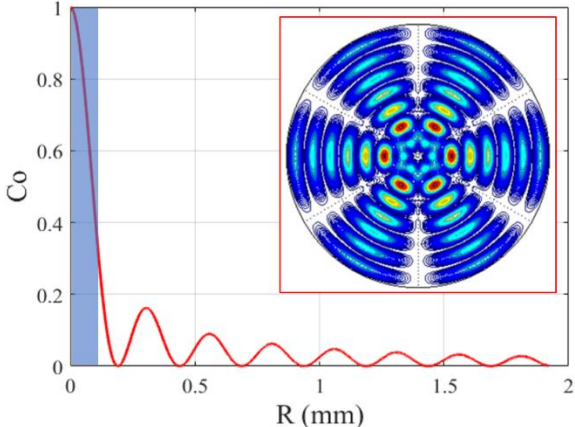
Fig.2. simulation emission current density, as a function of applied electric field. Inset: equivalent simulation structure of dual Ni80Cr20 alloy wires.

The proposed electron-optical system outlined here is a candidate for use in a 0.6 THz third harmonic  $\text{TE}_{37}$  mode gyrotron oscillator. According to gyrotron linear theory, the coupling expression depicted the electron beams interaction with the high frequency field is given by

$$C_o = \frac{J_{n-s}^2(K_{n,p}R_0)}{J_n^2(v_{n,p})(1-n^2/v_{n,p}^2)} \quad (2)$$

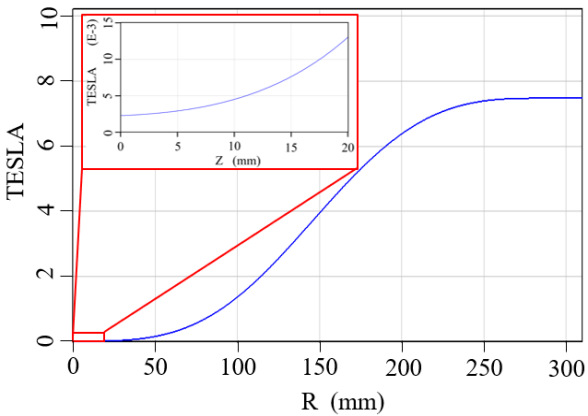
where  $s$  and  $v_{n,p}$  are the  $p^{\text{th}}$  root of  $J_n'(x)$  and the harmonic number, respectively.  $k_{n,p} = c_{n,p}/R_0$ .  $R_0$  is the guide center radius of the electron beam. In order to increase the coupling coefficient in the 0.6 THz third harmonic gyrotron,  $n=s$ , ensuring that the  $\text{TE}_{3n}$  mode is selected for higher coupling

1 coefficient. The normalized beam-wave coupling coefficient  
 2 as a function of beam radius is depicted in Fig. 3.



17 Fig.3. normalized beam-wave coupling coefficient as a function of beam  
 18 radius (the abscissa of the shaded region represents the radius of the electron  
 19 beam of the electron-optical system, which ranges from  $3\mu\text{m}$ - $110\mu\text{m}$ ). Inset:  
 20 diagram of  $\text{TE}_{37}$  mode.

21 As shown in Fig.3, the guiding center radius of the electron  
 22 beam is  $57\mu\text{m}$ , and the corresponding normalized coupling  
 23 coefficient is 0.77. In simulations the 9.2 T superconducting  
 24 magnetic system has been adopted, with the maximum value  
 25 of the magnetic field being 7.45 T, and the magnetic field in  
 26 the emission area is about 2.5 mT. Fig. 4 shows the  
 27 distribution of the magnetic field along the central axis, and the  
 28 final design parameters of the CNT cold-cathode electron-  
 29 optical system are listed in TABLE I.



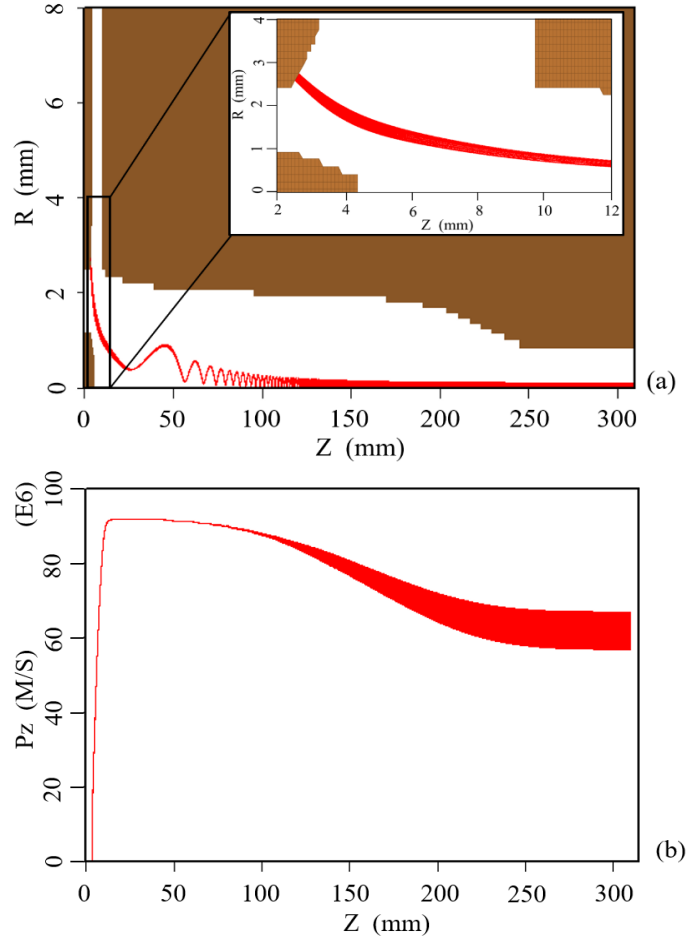
44 Fig. 4. Profile of the magnetic field intensity along the center axis. Inset:  
 45 magnetic field intensity local to the cathode.

46 TABLE I  
 47 Design parameters of the electron-optical system

48 Symbols	49 Parameters	50 Values and 51 Units
$V_a$	control anode voltage	-22.16 kV
$V_b$	Accelerating voltage	-23.5 kV
$B_c$	Magnetic field in the cathode area	25 mT
$B_0$	Magnetic field at output port of the electron-optical system	7.45 T
$R_k$	Average radius of emitter	2.74 mm
$R_0$	Guiding center radius of the electron beam	$57\mu\text{m}$
$I_b$	Beam current	160 mA

$J$	Emission current density	4.65 A/cm <sup>2</sup>
$\beta z$	Parallel velocity spread	8.9%
$\beta_\perp$	Perpendicular velocity spread	6.7%
$V_\perp / V_z$	Velocity ratio	1.1

1 The electron beam trajectory is shown in Fig. 5(a). The  
 2 parallel and perpendicular momentum of the electron beam as  
 3 a function of axial distance are shown in Figs. 5 (b) and 5 (c),  
 4 respectively. From the simulation results, in Fig. 5, when the  
 5 electron beam reaches  $z = 50$  mm, the parallel momentum of  
 6 the electron beam gradually decreases. On the contrary, the  
 7 perpendicular momentum tends to gradually increase, and  
 8 finally the speed tends to stabilize after the compression stage.  
 9 The simulation results show that the perpendicular and parallel  
 10 velocity spread of the electron beam are 6.7% and 8.9%,  
 11 respectively. The velocity ratio of the electron beam is 1.1, and  
 12 the beam current is 160 mA. These simulation results show that  
 13 a near-axis small orbit electron beam can be generated by the  
 14 developed electron-optical system, which makes an important  
 15 contribution to the control of mode competition in 0.6 THz  
 16 third harmonic  $\text{TE}_{37}$  mode gyrotrons.



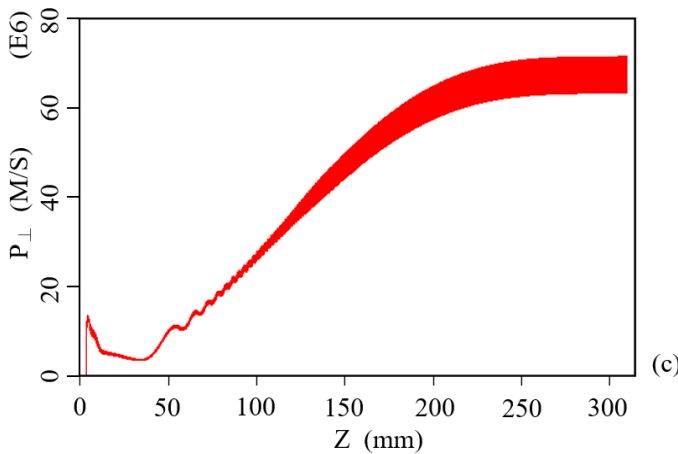


Fig. 5. (a) electron beam trajectory as a function of axial distance. Inset: detailed view of the electron beam in cathode area. (b) parallel momenta and (c) perpendicular momenta as a function of axial distance.

Design sensitivity to the magnetic field local to the cathode and the control anode voltage have been investigated in Fig. 6 (a) and Fig. 6 (b), respectively. In Fig. 6 (a), the velocity ratio and parallel velocity spread increase as the magnetic field in cathode volume and control anode voltage increase. On the contrary, the perpendicular velocity spread decreases. When the magnetic field in the immediate cathode locality is higher than 6 mT, the parallel velocity spread and velocity ratio increase rapidly.

Fig. 6 (b) shows that the control anode voltage modulates significantly operation of the electron-optical system. In order to generate the electron beam which can satisfy the necessary high current density in slow wave devices, the velocity ratio and the parallel velocity spread can be decreased as low as 0.44 and 4.7%, respectively, by adjusting control anode voltage.

Fig. 7 shows the electron beam trajectory and detailed view of the electron beam at the output port of the electron-optical system (control anode voltage  $V_a = -22.36$  kV). The radius of the electron beam is 80  $\mu$ m. The electron beam current and the emission current density are 123 mA and 3.57 A/cm<sup>2</sup>, respectively. The parallel energy account for 84% of the total energy, and the current density of the electron beam at the output port of the electron-optical system is about 620 A/cm<sup>2</sup>,

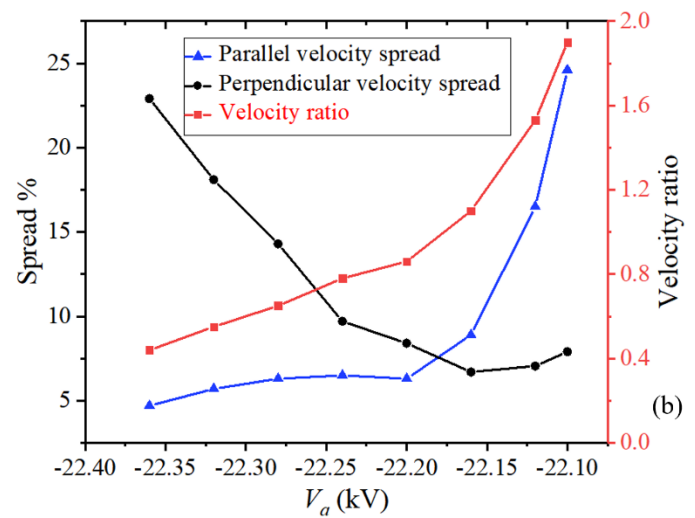
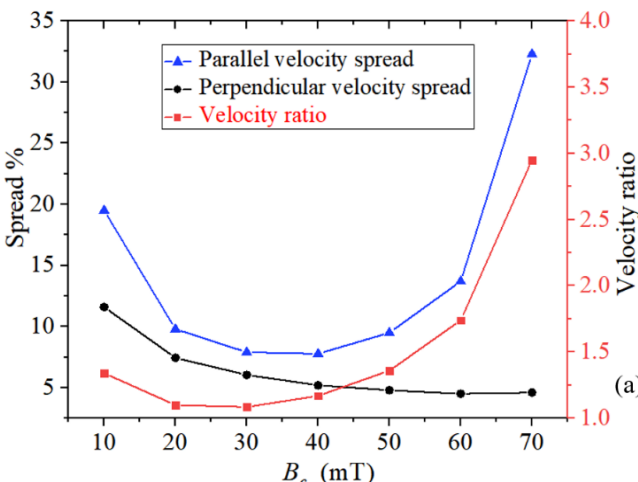


Fig. 6. (a) Design sensitivity to the magnetic field in cathode area. (b) Design sensitivity to the control anode voltage.

with the electron beam cross-sectional area compressed by 174 times, supporting the generation of the required high beam current densities for terahertz slow wave devices.

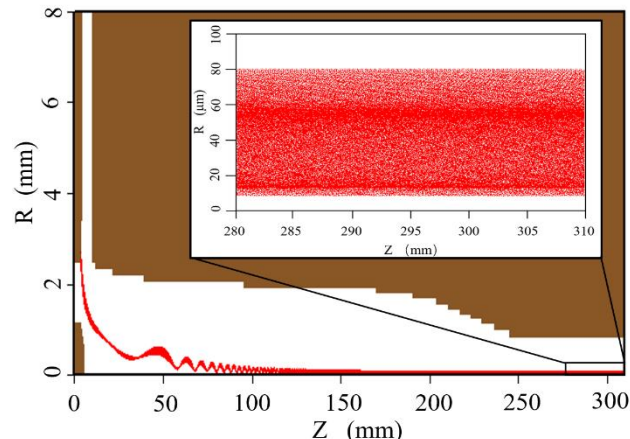


Fig. 7 electron beam trajectory as a function of axial distance (control anode voltage  $V_a = -22.36$  kV). Inset: detailed view of the electron beam at the output port of the electron-optical system.

### III. CONCLUSION

A high-current-density terahertz electron-optical system, suited for use in fast and slow wave devices, based on a CNT cold cathode has been developed. Mode competition can be well solved by means of the near-axis electron beam in high order harmonic gyrotrons. Modulation of the control anode voltage has been demonstrated, providing an effective approach to improving the current density. Current density up to 1300 A/cm<sup>2</sup> can be realized if the emission current density increases to the maximum experimental emission current density of 7.65 A/cm<sup>2</sup>. The electron-optical system provides a promising perspective for the development of terahertz radiation source based on CNTs and other emerging nanomaterials.

## REFERENCE

[1] J. H. Booske, Dobbs, Joye, Kory, Neil, Gun-Sik Park, Jaehun Park, and Temkin. "Vacuum Electronic High Power Terahertz Sources." *IEEE Transactions on Terahertz Science and Technology*, vol. 1, no.1, pp. 54-75, October. 2011, doi: 10.1107/s10762-011-9766-9.

[2] R.K Parker, R.H Abrams, B.G Danly, and B. Levush. "Vacuum Electronics." *IEEE Transactions on Microwave Theory and Techniques*, vol. 50, no. 3, pp. 835-845, March. 2002, doi: 10.1109/22.989967.

[3] R. J. Barker and E. Schamiloglu, "High-Power Microwave Sources and Technologies." Wiley-IEEE Press, 2001.

[4] V. L. Bratman, A. A. Bogdashov, G. G. Denisov, M. Yu Glyavin, Yu K. Kalynov, A. G. Luchinin, V. N. Manuilov, V. E. Zapevalov, N. A. Zavolsky, V. G. Zorin. "Gyrotron development for high power THz technologies at IAP RAS," *Journal of Infrared, Millimeter and Terahertz Waves*, vol. 33, no. 7, pp. 715-723, July. 2012, doi: 10.1007/s10762-012-9898-6.

[5] Chaojun Lei, Sheng Y u, Hongfu Li, Xinjian Niu, Qixiang Zhao, Y usheng Zhao, and Jiansheng Wang. "Analysis of a 0.6-THz Second Harmonic Gyrotron With Gradually Tapered Cavity." *IEEE Transactions on Plasma Science*, vol. 42, no. 2, pp. 293-299, February. 2014, doi: 10.1109/TPS.2013.2295654.

[6] Nusinovich, Gregory S, Thumm, Manfred K. A, Petelin, Michael I. "The Gyrotron at 50: Historical Overview." *Journal of Infrared Millimeter and Terahertz Waves*, vol. 35, no. 4, pp. 325-381, April. 2014, doi: 10.1007/s10762-014-0050-7.

[7] Nusinovich, Gregory S. "Remote Detection of Concealed Radioactive Materials by Using Focused Powerful Terahertz Radiation." *Journal of Infrared Millimeter and Terahertz Waves*, vol. 37, no. 6, pp. 515-535, June. 2016, doi: 10.1007/s10762-016-0243-3.

[8] Manfred K. A. Thumm. "Progress in gyrotron development." *Fusion Engineering and Design*, vol. 66-68, pp. 69-90, September. 2003, doi: 10.1016/S0920-3796(03)00132-7.

[9] Manfred K. A. Thumm. "Recent Developments on High-Power Gyrotrons—Introduction to This Special Issue." *Journal of Infrared Millimeter and Terahertz Waves*, vol. 32, no. 3, pp. 241-252, March. 2011, doi: 10.1007/s10762-010-9754-5

[10] M. Yu. Glyavin, N. A. Zavolskiy, A. S. Sedov, G. S. Nusinovich. "Low-voltage gyrotrons." *Physics of Plasmas*, vol. 20, no. 3, March. 2013, doi: 10.1063/1.4791663.

[11] M. Yu. Glyavin, V.N. Manuilov, G.G. Sominiskii, E.P. Taradaev, T.A. Tumareva. "The concept of an electron-optical system with field emitter for a spectroscopic gyrotron." *Infrared Physics & Technology*, vol. 78, pp. 185-189, September 2016, doi: 10.1016/j.infrared.2016.08.006.

[12] Ilya V. Bandurkin, Vladimir L. Bratman, Yury K. Kalynov, Ivan V. Osharin, and Andrei V. Savilov. "Terahertz Large-Orbit High-Harmonic Gyrotrons at IAP RAS: Recent Experiments and New Designs." *IEEE Transactions on Electron Devices*, vol. 65, no. 6, pp. 2287-2293, June. 2018, doi: 10.1109/TED.2018.2797311.

[13] V.L. Bratman, Yu. K. Kalynov, V.N. Manuilov, "Large-orbit gyrotron operation in the terahertz frequency range," *Physics Review Letter*, vol. 102, no. 24, June. 2009, doi: 10.1103/PhysRevLett.102.245101

[14] Xuesong Yuan, Ying Lan, Chunyan Ma, Yu Han, and Yang Yan. "Theoretical study on a 0.6 THz third harmonic gyrotron." *Physics of Plasmas*, vol. 18, no. 10, October. 2011, doi: 10.1063/1.3647564.

[15] K. Mizuno, and S. Ono. "Comment on Traveling Wave Oscillations in the Optical Region: A Theoretical Examination." *Journal of Applied Physics*, vol. 46, no. 4, pp. 1849, April. 1975, doi: 10.1063/1.321757.

[16] Seong-Tae Han, Seok-Gy Jeon, Young-Min Shin, Kyu-Ha Jang, Jin-Kyu So, Jong-Hyun Kim, Suk-Sang Chang, and Gun-Sik Park. "Experimental Investigations on Miniaturized High-frequency Vacuum Electron Devices." *IEEE Transactions on Plasma Science*, vol. 33, no. 2, pp. 679-684, April. 2005, doi: 10.1109/TPS.2005.844529.

[17] Carol Korya, Michael Reada, John Booskeb, Lawrence Ivesa, Giri Venkataramanb, David Marsdena and Sean Sengeleb. "650 GHz Traveling Wave Tube Amplifier." *33rd International Conference on Infrared, Millimeter and Terahertz Waves*. September 2008. doi: 10.1109/ICIMW.2008.4665623

[18] Qingyun Chen, Xuesong Yuan, Matthew T. Cole, Yu Zhang, Lin Meng, and Yang Yan. "Theoretical Study of a 0.22 THz Backward Wave Oscillator Based on a Dual-Gridded, Carbon-Nanotube Cold Cathode." *Applied Sciences*, vol. 8, no. 12, pp. 2462, December 2018, doi: 10.3390/app8122462.

[19] Xuesong Yuan, Yu Zhang, Matthew T. Cole, Yang Yan, Xiaoyun Li, Richard Parmee, Jianqiang Wu, Ningsheng Xu, William I. Milne, Shaozhi Deng. "A Truncated-cone Carbon Nanotube Cold-cathode Electron Gun." *Carbon*, vol. 120, pp. 374-379, August. 2017, doi: 10.1016/j.carbon.2017.03.046.

[20] Xuesong Yuan, Yu Zhang, Huan Yang, Xiaoyun Li, Ningsheng Xu, Shaozhi Deng, and Yang Yan. "A Gridded High-Compression-Ratio Carbon Nanotube Cold Cathode Electron Gun." *IEEE Electron Device Letters*, vol. 36, no. 4, pp. 399-401, April. 2015, doi: 10.1109/LED.2015.2401593.

[21] K. B. K. Teo et al., "Microwave devices: Carbon nanotubes as cold cathodes," *Nature*, vol. 437, no. 7061, pp. 968, October. 2005, doi: 10.1038/437968a.

[22] Xuesong Yuan, Weiwei Zhu, Yu Zhang, Ningsheng Xu, Yang Yan, Jianqiang Wu, Yan Shen, Jun Chen, Juncong She, Shaozhi Deng, "A fully-sealed carbon-nanotube cold-cathode terahertz gyrotron." *Scientific Report*, vol. 6, September. 2016, doi:10.1038/srep32936.

[23] Hae Jin Kim, Jin Joo Choi, Jae-Hee Han, Jae Hong Park, and Ji-Beom Yoo. "Design and Field Emission Test of Carbon Nanotube Pasted Cathodes for Traveling-wave Tube Applications." *IEEE Transactions on Electron Devices*, vol. 53, no. 11, pp. 2674-2680, November. 2006, doi:10.1109/TED.2006.884076.

[24] G. Ulisse, Francesca Brunetti, Emanuela Tamburri, Silvia Orlanducci, Matteo Cirillo, Maria Letizia Terranova, and Aldo Di Carlo. "Carbon nanotube cathodes for electron gun," *IEEE Electron Device Lett*, vol. 34, no. 5, pp. 698-700, May. 2013, doi: 10.1109/LED.2013.2250247.

[25] G. Ulisse, F. Brunetti, and A. Di Carlo, "Study of the influence of transverse velocity on the design of cold cathode-based electron guns for terahertz devices," *IEEE Transaction on Electron Devices*, vol. 58, no.9, pp. 3200-3204, September 2011,doi:10.1109/TED.2011.2158437.

[26] Yahachi Saito, Sashiro Uemurab, "Field emission from carbon nanotubes and its application to electron sources." *Carbon*, vol. 38, no. 2, pp. 169-182, 2000. doi: 10.1016/S0008-6223(99)00139-6.

[27] Yifan Zu, Xuesong Yuan, Xiaotao Xu, Matthew T. Cole, Yu Zhang, Hailong Li, Yong Yin, Bin Wang and Yang Yan. "Design and Simulation of a Multi-Sheet Beam Terahertz Radiation Source Based on Carbon-Nanotube Cold Cathode. *Nanomaterials*. vol 9, no. 12, December. 2019, doi: 10.3390/nano9121768.

[28] Wei Lei, Zhuoya Zhu, Chunyi Liu, Xiaobing Zhang, Baoping Wang, Arokia Nathan. "High-current field-emission of carbon nanotubes and its application as a fast-imaging X-ray source." *Carbon*, vol. 94, pp.687-693, November. 2015. doi: 10.1016/j.carbon.2015.07.044.

[29] Yunsong Di, Mei Xiao, Xiaobing Zhang, Qilong Wang, Chen Li, Wei Lei, and Yunkang Cui. "Large and stable emission current from synthesized carbon nanotube/fiber network." *Journal of applied physics*. vol. 5, no. 6, February. 2014. doi: 10.1063/1.4864431.

[30] Xiao-Lu Yan, Yu-Long Wu, Bao-Shun Wang, Quan Zhang, Rui-Ting Zheng, Xiao-Ling Wu, and Guo-an Cheng. "Fabrication of Carbon Nanotube on Nickel-chromium Alloy Wire for High-current Field Emission." *Applied Surface Science* vol. 450, pp. 38-45, August. 2018, doi: 10.1016/j.apsusc.2018.04.114.

[31] Xiaotao Xu, Xuesong Yuan, Qingyun Chen, Matthew T. Cole, Yu Zhang, Jie Xie, Yong Yin, Hailong Li, and Yang Yan. "A Low-Voltage, Pre-Modulation Terahertz Oscillator Based on a Carbon Nanotube Cold-Cathode". *IEEE Transaction on Electron Devices*. vol. 67, no. 3, pp.1266-1269, March. 2020, doi: 10.1109/TED.2020.2968932.